Volume 14-Issue 4 (2025)

Journal of Transportation Science and Technology

Journal homepage: https://tapchicongnghegtvt.vn

Adaptive Neural Network-Based Nonlinear Control of Quadcopters

Dang Xuan Ba[1], Le Manh Thang[2,3*], and Doan Van Dong[2,3]

[1]*Department of Automatic Control, HCMC University of Technology and Education (HCMUTE), HCM City, 70000 Vietnam*

[2]*Institute of Mechanical Engineering, University of Transport Ho Chi Minh City, HCM City, 70000 Vietnam.*

[3]*BRIDGE Research Group, University of Transport Ho Chi Minh City, HCM City, 70000 Vietnam.*

Keywords:
Quadcopter, Adaptive Control, RBF Neural Network, Estimating Disturbance.

ABSTRACT

This paper presents a novel adaptive neural network control strategy for trajectory tracking control of quadcopters in the presence of external disturbances and model uncertainties. The proposed method utilizes a hierarchical control structure, where an outer position loop is structured from a basic sliding mode controller (SMC), and the inner-loop attitude control is comprised of a backstepping approach and an adaptive Radial Basis Function (RBF) neural network. The RBF neural network is designed to approximate lumped disturbances in real time through Gaussian basis functions and an online weight adaptation law, eliminating the need for detailed disturbance modeling. To evaluate the performance of the proposed approach, we conduct comparative simulations against a SMC controller and a Robust Feedback Linearization (RFBL) control method. Results obtained demonstrate that the RBF-based controller achieves superior tracking accuracy, faster convergence, and improved disturbance rejection, particularly under time-varying and uncertain conditions. These findings highlight the potential of adaptive learning-based controllers for robust and model-free UAV applications.

1. Introduction

Unmanned Aerial Vehicles (UAVs), especially quadcopters, are widely used in modern applications ranging from aerial surveillance and mapping to delivery systems as well as search-and-rescue missions [1]. However, their working performances remain significant challenges due to the systematic nonlinear dynamics, underactuated structures, and high sensitivity to external disturbances such as wind or modeling inaccuracies. Numerous control strategies have been proposed to tackle these issues, including Proportional-Integral-Derivative (PID) controllers thanks to simplicity and acceptable control outcomes [2]–[3]. Its advanced versions have been studied to enhance the control quality [4]–[9]. To address optimal control problems in UAV systems, Linear Quadratic Regulator (LQR) methods are widely recognized as effective solutions [10]. Compared to classical PID controllers, the LQR approaches require more mathematical computation to determine full-state feedback matrices by minimizing quadratic cost functions derived from system dynamics. Various improvements have been considered to improve reliability of the LQR-based control systems, such as integrating state observers for attitude estimation [11] or combining with feedback linearization for position tracking [12]. These enhancements have yielded better control accuracies, but their control robustness could be degraded in some cases [13]–

* Le Manh Thang. Institute of Mechanical Engineering, University of Transport Ho Chi Minh City, HCM City, 70000 Vietnam
Email: thang.le@ut.edu.vn

https://www.doi.org/10.55228/JTST140411
Recieved: April 26, 2025; Recieved in revised: June 30, 2025; Accepted: July 14, 2025
Available online: July 15, 2025
pISSN: 1859-4263; eISSN: 3030-4261

[14]. This drawback created motivation for nonlinear control approaches designed for the UAV systems.

To handle nonlinearities in quadcopter dynamics, backstepping-based control approaches have been extensively studied. In [15]–[16], mathematical models of quadrotor systems were developed, and backstepping-based PID strategies were designed for attitude and altitude subsystems. Their effectiveness was demonstrated through both theoretical analysis and simulation results. However, the control performances could be further improved by dealing uncertainties of the system models. As a result, adaptive backstepping methods have been proposed, with adaptation laws derived either from system models [13], [17] or based on intelligent learning frameworks such as neural networks [18].

Compared to backstepping control techniques, sliding mode controllers (SMC) offer a simpler design framework and are widely appreciated for their robustness against system uncertainties [14]. Early SMC-based designs demonstrated effective stabilization and disturbance rejection in quadrotor systems [19], [20], though they often suffered from high-frequency chattering and lacked adaptability. To improve performance, adaptive SMC strategies were introduced, allowing real-time adjustment of control gains to handle system variations more effectively [21]–[28]. Moreover, intelligent learning mechanisms have been integrated into terminal SMC frameworks using RBF neural networks, achieving finite-time convergence in both position and attitude tracking by approximating unknown dynamics and external disturbances. However, chattering was still observed in attitude responses [29]. Recently, a robust disturbance observer-based control framework combined with advanced sliding mode control methods to enhance robustness and finite-time convergence under model uncertainties [30].

Motivated by these challenges, this paper proposes an adaptive RBF neural network-based nonlinear controller for quadcopters, aiming to combine the strengths of nonlinear control and adaptive learning technology. The RBF neural network is embedded within a backstepping framework to estimate and cancel out unknown disturbances in real time. Unlike previous RFLB methods, the proposed controller does not require precise modeling of disturbances or system parameters. To validate the proposed approach, comprehensive comparative simulations were conducted under various tracking scenarios and disturbance conditions.

The rest of the paper is organized as follows. Section 2 reviews the system modeling and discusses the control objective. Section 3 details the design of the adaptive RBF neural network-based nonlinear controller. Section 4 shows comparative simulation results and performance analysis. Finally, the remarks and directions for future work are concluded in section 5.

2. System Modeling and Control Objectives

Overview of the quadcopter system with a world frame **{W}** and body-fixed frame **{B}** is presented in Figure. 1. The motion of the UAV is governed by the speed variation of its four motors. The dynamical model of the Quadcopter in the air under external disturbances is given as [6], [27]:

$$\begin{cases} \ddot{x} = \dfrac{u_1}{m}\left(s_\theta c_\phi c_\psi + s_\phi s_\psi\right) \\ \ddot{y} = \dfrac{u_1}{m}\left(s_\theta c_\phi s_\psi - s_\phi c_\psi\right) \\ \ddot{z} = \dfrac{u_1}{m}\left(c_\theta c_\phi\right) - g \\ \ddot{\phi} = \dfrac{I_y - I_z}{I_x}\dot{\theta}\dot{\psi} - I_m\dfrac{\dot{\theta}}{I_x}\Omega_\psi + \dfrac{u_2}{I_x} + d_\phi \\ \ddot{\theta} = \dfrac{I_z - I_x}{I_y}\dot{\phi}\dot{\psi} + I_m\dfrac{\dot{\phi}}{I_y}\Omega_\psi + \dfrac{u_3}{I_y} + d_\theta \\ \ddot{\psi} = \dfrac{I_x - I_y}{I_z}\dot{\phi}\dot{\theta} + \dfrac{u_4}{I_z} + d_\psi \end{cases} \quad (1)$$

where x, y, z [m] and ϕ, θ, ψ [rad] are respectively the position and Euler angles relative to the world frame **{W}**; $I_{x,y,z}$ [kg.m^2] represent the inertia moment of the quadrotor in x, y, z directions , I_m [kg.m^2] is the inertia moment of the actuators , m [kg] is the total mass of the quadrotor , Ω_ψ [rad/s] is the difference between the angular velocities of rotors, $d_\phi, d_\theta, d_\psi \in \mathbb{R}$ [rad/s^2] denote lumped disturbances that are combined from modeling errors and the external disturbances affecting the system dynamics, $g = 9.8 m/s^2$ is the gravitational acceleration, u_1 [N] is the virtual translational control signal, and u_2, u_3 and u_4 [N.m] are respectively the virtual rotational control signals for the roll, pitch and yaw directions. Several common notations are defined as $c(\bullet) \triangleq \cos(\bullet)$ and $s(\bullet) \triangleq \sin(\bullet)$.

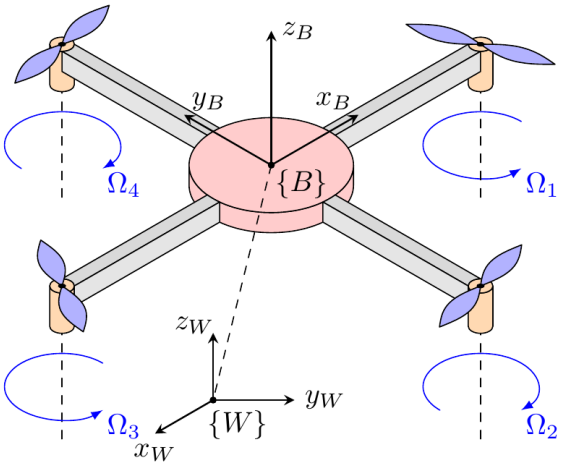

Figure 1. Configuration of the UAV system.

The virtual control signals $u_{i|i=1...4}$ and the variation effect (Ω_ψ) are synthesized from angular velocities of rotors [23], [25], as follows:

$$\Omega_\psi = \Omega_1 - \Omega_2 + \Omega_3 - \Omega_4 \tag{2}$$

$$\begin{bmatrix} u_1 \\ u_2 \\ u_3 \\ u_4 \end{bmatrix} = \begin{bmatrix} l\cdot k & l\cdot k & l\cdot k & l\cdot k \\ 0 & -l\cdot k & 0 & l\cdot k \\ -l\cdot k & 0 & l\cdot k & 0 \\ -b & b & -b & b \end{bmatrix} \begin{bmatrix} \Omega_1^2 \\ \Omega_2^2 \\ \Omega_3^2 \\ \Omega_4^2 \end{bmatrix} \tag{3}$$

where $\Omega_{i|i=1...4}$ are respectively velocities of the respective rotors, k [Ns²] is thrust coefficient, b [Nms²] is drag coefficient, l [m] is the frame radius of the quadrotor.

Remark 1: The control objective of the paper is to derive proper smooth control signals to force the system outputs follow desired position trajectories (x_d, y_d, z_d) and a desired yaw angle (ψ_d). However, the complicated cross-coupling structural characteristics, uncertainties and external disturbances in the system dynamics are main obstacles restricting the expected control performances [26]–[28].

3. An Adaptive RBF Neural Network Based Nonlinear Controller

To effectively realize the control mission, the proposed controller is structured with two control layers: altitude control layer and attitude control layer. The altitude control layer is structured with a simple yet effective control framework, while the angle control layer has to be designed with an advanced control technique to deal with internal and external disturbances during the system working.

3.1. Altitude Control Layer

The purpose of this control layer is to derive virtual control signals to drive the system position (x, y, z) to a desired position (x_d, y_d, z_d). We first consider the altitude dynamics of the system (1):

$$\begin{cases} \ddot{x} = \dfrac{u_1}{m}(s_\theta c_\phi c_\psi + s_\phi s_\psi) \\ \ddot{y} = \dfrac{u_1}{m}(s_\theta c_\phi s_\psi - s_\phi c_\psi) \\ \ddot{z} = \dfrac{u_1}{m} c_\theta c_\phi - g \end{cases} \tag{4}$$

Currently, the separated dynamics are too complicated to find the best control signal. The system (4) could be rewritten in a simpler form to facilitate the design process,

$$\begin{bmatrix} \ddot{x} \\ \ddot{y} \\ \ddot{z} \end{bmatrix} = \begin{bmatrix} u_x \\ u_y \\ u_z \end{bmatrix} \equiv \begin{bmatrix} s_\theta c_\phi c_\psi + s_\phi s_\psi \\ s_\theta c_\phi s_\psi - s_\phi c_\psi \\ c_\theta c\phi \end{bmatrix} \frac{u_1}{m} - \begin{bmatrix} 0 \\ 0 \\ g \end{bmatrix} \tag{5}$$

where u_x, u_y and u_z are respectively virtual control signals along x, y, z directions.

We next define the following altitude control errors:

$$\begin{cases} e_x = x - x_d \\ e_y = y - y_d \\ e_z = z - z_d \end{cases} \tag{6}$$

To force the control error in (6) to be zero from the dynamics (5), the following sliding surfaces could be employed as a simplest-yet-effective control method:

$$\begin{cases} s_x = \dot{e}_x + k_{1x} e_x \\ s_y = \dot{e}_y + k_{1y} e_y \\ s_z = \dot{e}_z + k_{1z} e_z \end{cases} \tag{7}$$

where k_{1x}, k_{1y}, k_{1z} are positive constants.

The virtual sliding mode control signals are easily resulted in from the conventional sliding mode control theories, as follows:

$$\begin{cases} u_x = \ddot{x}_d - k_{1x}\dot{e}_x - k_{2x}s_x \\ u_y = \ddot{y}_d - k_{1y}\dot{e}_y - k_{2y}s_y \\ u_z = \ddot{z}_d - k_{1z}\dot{e}_z - k_{2z}s_z \end{cases} \quad (8)$$

where k_{2x}, k_{2y}, k_{2z} are positive constants.

Remark 2: Applying the control signal (8) to the system (6) can make the sliding surfaces converge to zero in infinite time. In fact, there are many control solutions to obtain high control accuracies for the objective (6) of the system (5). Here, the conventional SMC method is selected due to the simplicity in implementation.

By using the cross-coupling behaviors in (5), proper control signals could be extracted from the virtual signal (8), as follows [17]–[23]:

$$\begin{cases} u_1 = \dfrac{u_z + g}{c_\theta c_\phi} m \\ \phi_d = \arcsin\left(\dfrac{m}{u_1}\left(u_x s_\psi - u_y \mathrm{c}_\psi\right)\right) \\ \theta_d = \arctan\left(\dfrac{u_x \mathrm{c}_\psi + u_y \mathrm{s}_\psi}{u_z + g}\right) \end{cases} \quad (9)$$

where ϕ_d, θ_d are the desired trajectories of the roll and pitch subsystems, respectively.

3.2. Attitude Control Layer

This subsection presents procedures to design the attitude control signals to realize the control objectives for the roll, pitch and yaw angles. Advanced control techniques are adopted in proper manners for the designing process.

3.2.1. Design of Yaw Angle Control

The yaw dynamics are considered from the system (1), as follows:

$$\ddot{\psi} = \frac{u_4}{I_z} + \tau_{\psi nn} \quad (10)$$

where $\tau_{\psi nn} = \dfrac{I_x - I_y}{I_z}\dot{\phi}\dot{\theta} + d_\psi$ denotes the lumped unknown term that is combined from internal and external disturbances.

Assumption 1: The lumped disturbance $(\tau_{\psi nn})$ and its time derivative are bounded [28], [30].

We here consider a control error of the yaw control mission:

$$e_\psi = \psi - \psi_d \quad (11)$$

For simplicity, one could realize the control objective (11) by a conventional SMC control framework as just presented in the previous section. The sliding surface of the yaw control is defined as

$$s_\psi = \dot{e}_\psi + k_{1\psi}e_\psi \quad (12)$$

where $k_{1\psi}$ is a positive constant.

The yaw control signal is then formulated based on the SMC and RBF neural network based nonlinear disturbance as follows:

$$\begin{cases} u_4 = I_z(\ddot{\psi}_d - k_{1\psi}\dot{e}_\psi - k_{2\psi}s_\psi - \tau_{\psi nn}) \\ \tau_{nn\psi} = \mathrm{w}_\psi^T \zeta_\psi \end{cases} \quad (13)$$

where w_ψ is learning weight vector and ζ_ψ is a vector of Gaussian activations functions.

3.2.2. Design of Roll and Pitch Angle Control

In this subsection, new low-level controllers are designed to control the roll and pitch angles follow the desired signals that have just been derived from the high-level controller. The control rules (8) and (9) reveal that the desired roll and pitch angles themselves contain high-order time derivatives. It means that one need a new special control algorithm for this control mission. As usual, we start by defining a roll control error:

$$e_\phi = \phi - \phi_d \quad (14)$$

From (1), the roll dynamics could be rewritten in a simpler form as

$$\ddot{\phi} = \frac{u_2}{I_x} + \tau_{nn\phi} \tag{15}$$

where $\tau_{nn\phi} = \frac{I_y - I_z}{I_x}\dot{\theta}\dot{\psi} - I_m \frac{\dot{\theta}}{I_x}\Omega_\psi + d_\psi$ denotes the lumped unknown disturbance of the roll dynamics that is combined from internal and external disturbances.

Assumption 2: The lumped disturbance $(\tau_{nn\phi})$ and its time derivatives are bounded.

The time derivative of the error (14) is

$$\dot{e}_\phi = \dot{\phi} - \dot{\phi}_d \tag{16}$$

A virtual control signal for the roll dynamics is selected as

$$u_{v1,\phi} = -k_{1\phi} e_\phi \tag{17}$$

where $k_{1\phi}$ is a positive constant.

The virtual control signal (17) is to compensate for the time derivatives in (16). We continue considering a new control error

$$e_{1,\phi} = \dot{\phi} - u_{v1,\phi} \tag{18}$$

Its time derivative in the context of the dynamics (15) is

$$\dot{e}_{1,\phi} = \frac{u_2}{I_x} + \tau_{d\phi} + k_{1\phi}\left(\dot{\phi} - \dot{\phi}_d\right) \tag{19}$$

To force the error (18) to zero or be as small as possible, the final control signal is selected as

$$\begin{cases} u_2 = I_x\left(-k_{1\phi}\dot{\phi} - k_{2\phi}e_\phi - \tau_{nn\phi}\right) \\ \tau_{nn\phi} = \mathrm{w}_\phi^T \zeta_\phi \end{cases} \tag{20}$$

where w_ϕ is learning weight vector and ζ_ϕ is a vector of the Gaussian activations function.

Effectiveness of the nonlinear disturbance-observer-based control signal (20) to the roll dynamics is investigated by the following statement.

3.2.3. Learning mechanism for RBF neural network weights

The performance of the RBF neural network controller largely depends on the accuracy of the neural network's ability to approximate unknown disturbance dynamics. To ensure real-time adaptation and robust performance, an online learning law is designed to update the RBF network weights continuously.

Let $\mathrm{w} \in \mathbb{R}^n$ be the vector of adaptive weights associated with the Gaussian basis functions

$$\zeta(x) = \exp\left(-\frac{(x - x_c)}{2\sigma^2}\right)^2 \tag{21}$$

Where x is state vector of the dynamics needing to estimate.

The network output, which estimates the disturbance, is defined as:

$$\tau_{nn\phi} = \mathrm{w}^T \zeta(x) \tag{22}$$

To ensure convergence and boundedness of the approximation error, the weight update law is selected based on a gradient descent strategy derived from Lyapunov stability considerations:

$$\dot{\mathrm{w}} = \gamma\, \zeta(x)\, s_{exc}(x) \tag{23}$$

where $\gamma \in \mathbb{R}^{n\times n}$ is a positive definite learning rate matrix, and $s_{exc}(x)$ denotes an excitation signal of the learning process. Structure of the excitation signal $s_{exc}(x)$ depends the nature of the control system. For instance, in the yaw control, the signal $s_{exc}(x)$ is the sliding surface (12) while in the roll control, $s_{exc}(x)$ is the new synthesize error (18). The inclusion of $s_{exc}(x)$ ensures that the learning mechanism is only active when tracking errors are present.

To improve robustness and prevent unnecessary adaptation in steady-state conditions, a dead zone threshold can be applied to the update law:

$$\dot{\mathrm{w}} = \begin{cases} \gamma\,\zeta(x)\,s_{exc}(x), & \text{if } |s_{exc}(x)| > \delta \\ 0, & \text{otherwise} \end{cases} \quad (24)$$

This structure avoids weight drift due to sensor noise or small fluctuations near equilibrium. By carefully tuning the learning rate matrix and the dead zone threshold, the RBF network achieves fast learning during transients and stability during steady-state tracking.

This learning mechanism is integrated into the control system without introducing discontinuous terms, preserving smooth control outputs and enabling high-performance adaptive control of quadcopter systems.

3.2.4. Closed-Loop system and Stability Discussion

To evaluate the stability of the proposed control architecture, we consider the closed-loop dynamics of the quadcopter's yaw subsystem under the influence of the adaptive RBF neural network.

Let $\mathrm{w}_0 \in \mathbb{R}^n$ be the ideal weight vector, which represents the optimal mapping from the RBF basis to the true disturbance, is unknown in practice. Then, actual disturbance is

$$\tau_{dl} = \mathrm{w}_0^T \zeta(x) \quad (25)$$

The adaptive learning law is designed to drive estimating weight w toward ideal weight w_0, thereby ensuring that the neural network output approximates the disturbance effectively over time.

Assuming the unknown disturbance can be approximated by the RBF network $\tau_{nn} = \mathrm{w}^T \zeta(x)$, the control input cancels out the estimated disturbance and drives to zero. The disturbance estimation is not perfect due to the difference between actual and estimated parameters. This gives rise to a residual disturbance:

$$\tau_{dl} - \tau_{nn} = \left(\mathrm{w}_0^T - \mathrm{w}^T\right)\zeta(x) = -\tilde{\mathrm{w}}^T \zeta(x) \quad (26)$$

where $\tilde{\mathrm{w}} = \mathrm{w} - \mathrm{w}_0$ is the estimation error between the current and ideal weight vector.

Substituting the control input into the system dynamics (12) and (13), the derivative of the sliding surface becomes:

$$\dot{s}_\psi = -k_{2\psi} s_\psi - \tilde{\mathrm{w}}^T \zeta_\psi \quad (27)$$

Now, an Lyapunov function is considered as

$$V_\psi = \frac{1}{2} s_\psi^2 + \frac{1}{2} \tilde{\mathrm{w}}^T \gamma_\psi^{-1} \tilde{\mathrm{w}} \quad (28)$$

Taking the time derivative of function (28) and applying the update law (23):

$$\begin{aligned} \dot{V}_\psi &= s_\psi \dot{s}_\psi + \tilde{\mathrm{w}}^T \gamma_\psi^{-1} \dot{\tilde{\mathrm{w}}} \\ &= s_\psi(-k_{2\psi} s_\psi - \tilde{\mathrm{w}}^T \zeta_\psi) + \tilde{\mathrm{w}}^T \gamma_\psi^{-1}(\gamma_\psi \zeta_\psi s_\psi) \\ &= -k_{2\psi} s_\psi^2 \end{aligned} \quad (27)$$

This shows that the closed-loop system is stable in the sense of Lyapunov.

Remark 3: Overview of the closed-loop control system is summarized in Figure. 2. The controller is designed based on a proper combination of a sliding-mode-backstepping control scheme and an adaptive RBF neural network for an asymptotic control performance without directly using any discontinuous function under time-varying disturbances. Its adaptation is activated by a nonlinear weight-learning mechanism.

4. Validation Results

This section presents verification results of the proposed controller for tracking control missions. Sliding-mode-control (SMC) methods and Robust Feedback Linearization (RFBL) controller [30] were also implemented to control the system for comparison purpose. The system parameters that are referred from previous work [1], [3] are shown in Table 1.

Table 1. Parameters of the system model

Parameters	Value (Unit)
I_x, I_y, I_z, I_m	0.00085 (kg.m^2)
m	1 kg
g	9.81 m/s^2
k	1.2338x10-5 (Ns^2)
b	1.27513x10-5 (Nms^2)
l	0.2 (m)

4.1. Case study 1: Basic verification

In the first simulation, the three controllers were performed in a very basic test without an external disturbance in which the desired positions and yaw angle were chosen to be $x_d = 0.7$ (m); $y_d = -0.9$ (m); $z_d = 2.0$ (m); $\psi_d = 0.5$ (rad). Validation results obtained by the controllers are shown in Figs. 3–6. Figures 3 and 4 show that the steady-state control errors of the three controllers were almost same (about 0.005 (m) for all directions).

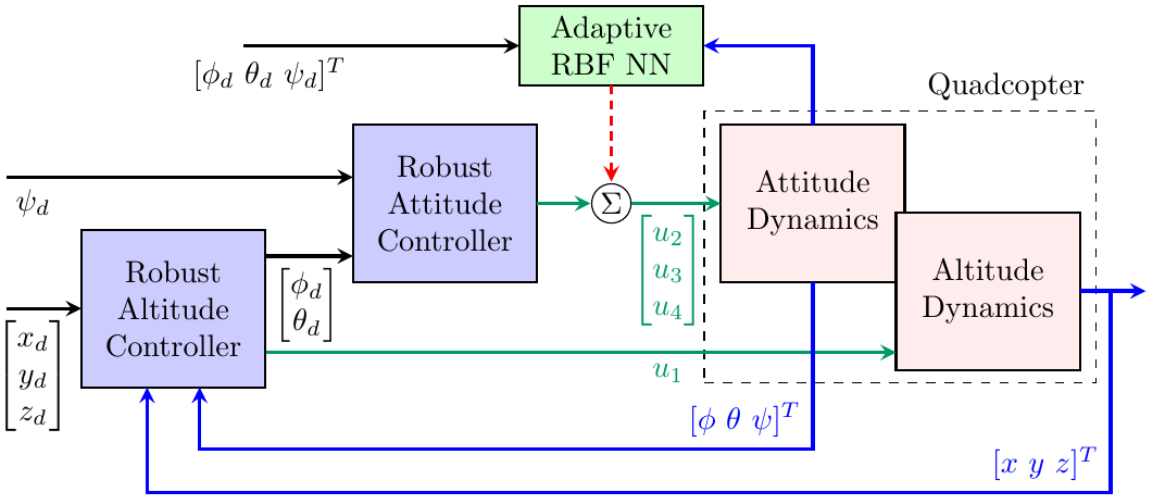

Figure 2. Block diagram of the proposed controller.

The transient responses of the nonlinear controllers (SMC, RFBL and the proposed ones) were not significantly different. The setting times of the nonlinear controllers were respectively about 2(s), 2(s), 1.5(s), and 0.8(s) for the *x, y, z* and yaw subsystems. The higher control performances of the SMC and proposed controllers came from the advantages of the nonlinear control design [26] – [28]. The RFBL controller provided satisfactory tracking but exhibited slight jitter in the roll and pitch responses, as seen in the attitude plots.

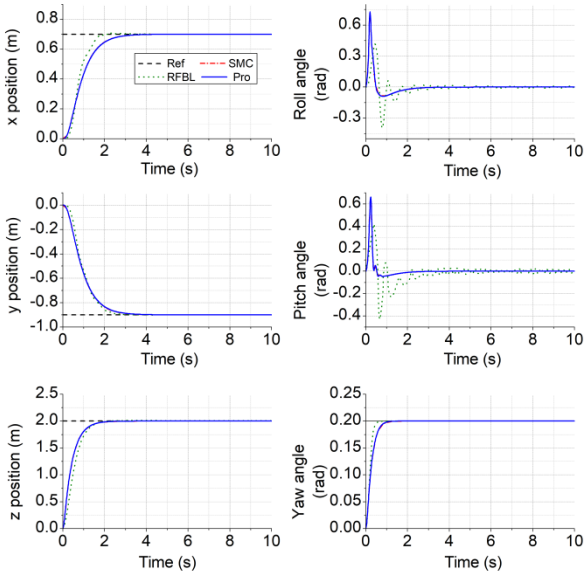

Figure 3. System responses in the case study 1.

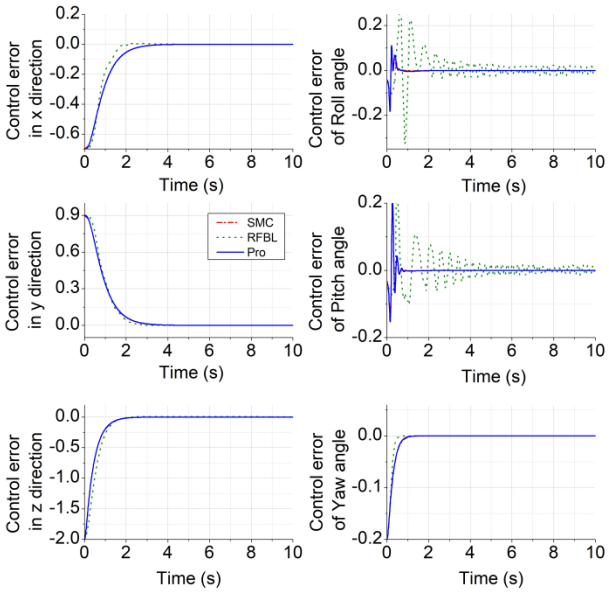

Figure 4. Control errors of the comparative controllers in the case study 1.

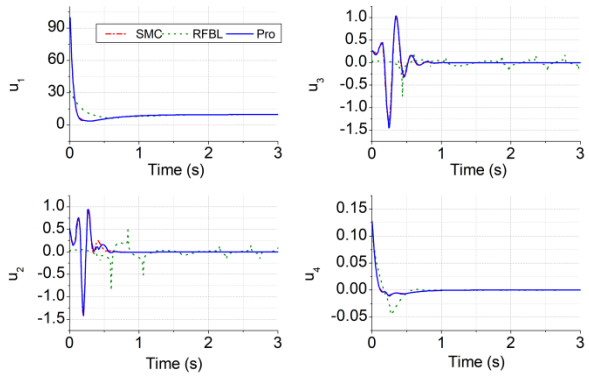

Figure 5. Control signals generated by theomparative controllers in the case study 1.

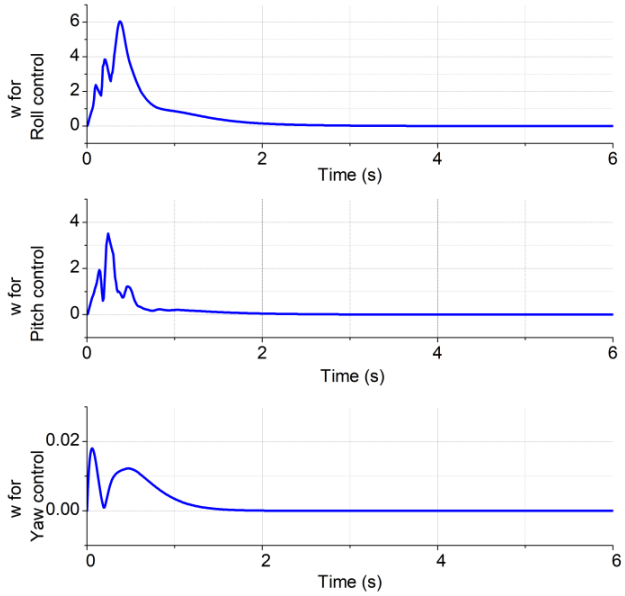

Figure 6. Variation of adaptive weights generated by the proposed controller in the case study 1.

Table 2. SMC controller parameters

CONTROLLER PARAMETERS	
Parameters	Value
$k_{SMCx}, k_{SMCy}, k_{SMCz}$	2.5; 2; 2
$k_{SMC1x}, k_{SMC1y}, k_{SMC1z}$	20; 2.5; 2.5
$k_{SMC\phi}, k_{SMC\theta}, k_{SMC\psi}$	5; 20; 20
$k_{SMC1\phi}, k_{SMC1\theta}, k_{SMC1\psi}$	50; 50; 15

4.2. Case study 2: Verification with stationary trajectories and external disturbances

In the second simulation, the controllers were further evaluated under more challenging conditions. New stationary reference setpoints were defined as $x_d = -1.5$ (m); $y_d = 2$ (m); $z_d = 3$ (m) and $\psi_d = -1.5$ (rad). Additionally, external disturbances were applied to the rotational dynamics, as shown in Fig. 7. These disturbances were intentionally designed with varying frequencies and amplitudes to emulate real-world environmental effects such as wind gusts or mechanical vibrations. The modeling assumption follows prior works [28], [30], where disturbances are treated as bounded, continuous, and persistently exciting, to test the robustness of adaptive controllers. After applying the same controllers to the system, their simulation results achieved are shown in Figs. 8–10. In the new working condition, without equipping any adaptation law, control precision of the SMC method has been reduced but still in acceptable ranges: the new SMC steady-state control error of the *y* direction was only 0.03 (m). Thanks to the use of the adaptive RBF neural network based nonlinear design, the proposed controller could maintain the good performance in the harder working condition: as seen in Fig. 9, the new steady-state control error of the y direction was stabilized at 0.005 (m). To this end, data plotted in Fig. 10 shows Root-Mean-Square value of the weight vectors were automatically adjusted at new levels. This confirms that the adaptive mechanism was effectively activated and reconfigured online to counteract the changing dynamics, a capability not available in the conventional SMC design.

Table 3. Robust Feedback Linearization (RFBL) controller parameters

CONTROLLER PARAMETERS	
Parameters	Value
$K_{pz}, K_{p\phi}, K_{p\theta}, K_{p\psi}, K_{px}, K_{py}$	3
$K_{dz}, K_{d\phi}, K_{d\theta}, K_{d\psi}, K_{dx}, K_{dy}$	6

Parameters	Value
$k_{1z}, k_{1\phi}$	7; 4
$k_{1\theta}, k_{1\psi}, k_{1x}, k_{1y}$	6
$k_{2\phi}$	1.1
$k_{2\phi}, k_{2x}, k_{2y}$	0.5; 0.6
$k_{2z}, k_{2\theta}, k_{2\psi}$	1
$c_1, c_2, c_3, c_4, c_5, c_6$	10

Table 4. Adaptive RFB neural network parameters

CONTROLLER PARAMETERS

Parameters	Value
n	8
$k_{1\phi}, k_{2\phi}, \gamma_\phi$	2; 1; 10
$k_{1\theta}, k_{2\theta}, \gamma_\theta$	3; 1; 30
$k_{1\psi}, k_{2\psi}, \gamma_\psi$	20; 0.5; 5

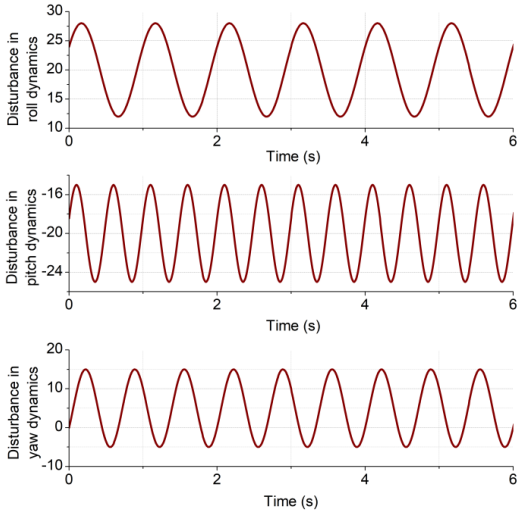

Figure 7. External disturbances affecting the drone in the case study 2.

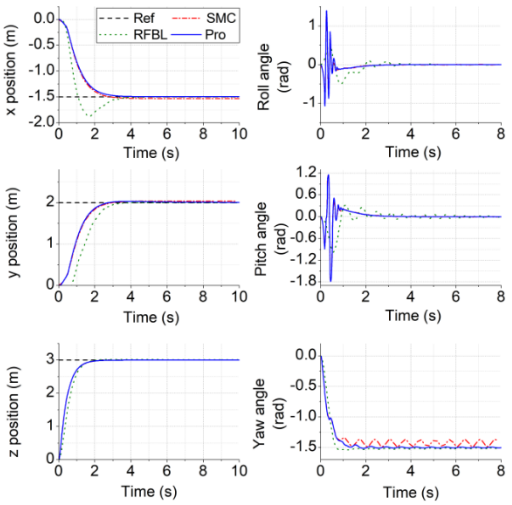

Figure 8. System responses in the case study 2.

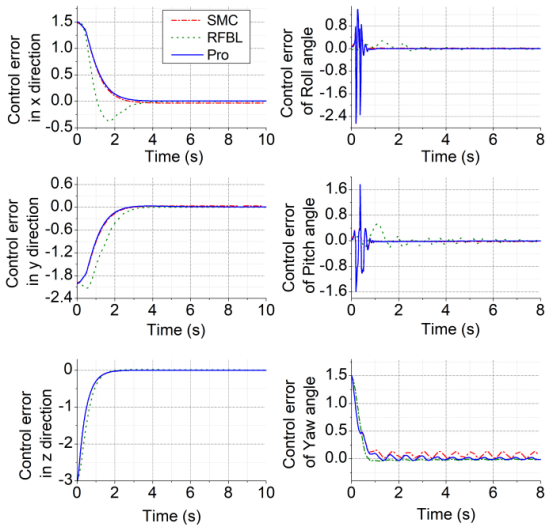

Figure 9. Control errors of the comparative controllers in the case study 2.

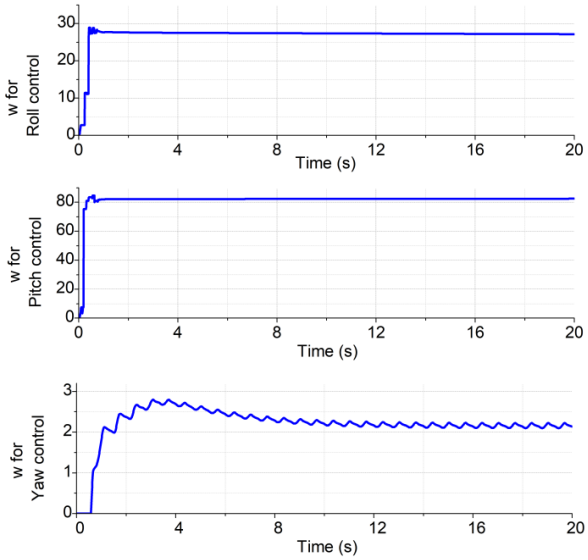

Figure 10. Variation of adaptive weights generated by the proposed controller in the case study 2.

5. Conclusion

This paper proposed an adaptive nonlinear control strategy for quadcopters based on an RBF neural network, aiming to enhance tracking performance under both nominal and disturbed conditions. Simulation results showed that the proposed controller achieved fast convergence and high accuracy in position and attitude tracking. Under basic test conditions, it outperformed the conventional SMC controller in terms of transient response and steady-state precision. When external harmonic disturbances were introduced, the proposed method maintained stable tracking with control quality comparable to the RFBL controller, while still

offering improved robustness and smoother attitude responses. In addition, the closed-loop stability of the yaw subsystem was rigorously proven using Lyapunov theory, validating the theoretical foundation of the control design. Overall, the proposed method demonstrates strong potential for reliable quadcopter control in dynamic and uncertain environments. Future work will focus on hardware-in-the-loop (HIL) testing and real-time implementation on physical quadcopters.

Contributions of authors in this article

Le Manh Thang: Methodology, Data management, Formal analysis, Investigation, Validation, Visualization, Grant acquisition, Feedback on peer review, Writing – original manuscript. **Dang Xuan Ba**: Data compilation, Data analysis, Investigation, Verification, Writing – original manuscript. **Doan Van Dong**: Investigation, Verification, and Overall Checking.

Declaration of competing interest and dedication to copyright

The authors declare the absence of any potential conflicts of interest from this study and affirm that the paper has not been previously published.

Data available

Data will or will not be provided upon request.

Acknowledgments

This work was supported by Ho Chi Minh City University of Technology and Education, Vietnam, under Grant T2024-01ĐH.

References

[1] S. Leal, C. Abeykoon, and S. Perera, "Design, Simulation, Analysis and Optimization of PID and Fuzzy Based Control Systems for a Quadcopter", *Electronics*, vol. 10, no. 18, pp. 2218, 2021, doi: 10.3390/electronics10182218

[2] A.T. Bayisa, "Controlling Quadcopter Altitude using PID-Control System", *Internation Journal of Engineering Research and Technology*, vol. 8, no. 12, pp. 195-199, 2019, Doi: 10.17577/IJERTV8IS120118.

[3] A. Chovancová, T. Fico, F. Duchon, M. Dekan, L. Chovanec and M. Dekanová, "Control Methods Comparison for the Real Quadrotor on an Innovative Test Stand", *Applied Sciences,* vol. 10, no. 6, pp. 2064, 2020, Doi: 10.3390/app10062064.

[4] M. F. Silva, A. C. Ribeiro, M. F. Santos, M. J. Carmo, L. M. Honório, E. J. Oliveira and V. F. Vidal, "Design of Angular PID Controllers for Quadcopters Built with Low-Cost Equipment", in 20th International Conference on System Theory, Control and Computing (ICSTCC), Sinaia, Romania, October 13-15, 2016, Doi: 10.1109/ICSTCC.2016.7790668

[5] N. Bao, X. Ran, Z. Wu, Y. Xue, K. Wang, "Research on attitude controller of quadcopter based on cascade PID control algorithm", in *2nd Information Technology, Networking, Electronic and Automation Control Conference (ITNEC)*, Chengdu, China, 2017, Doi: 10.1109/ITNEC.2017.8285044

[6] M. Rabah, A. Rohan, S. A. S. Mohamed, and S. H. Kim, "Autonomous moving target-tracking for a UAV quadcopter based on fuzzy-PI," *IEEE Access,* vol. 7, pp. 38407-38419, 2019, Doi: 10.1109/ACCESS.2019.2906345.

[7] I. Matei, C. Zeng, S. Chowdhury, R. Rai, and J. Kleer, "Controlling draft interactions between quadcopter unmanned aerial vehicles with physics-aware modeling," *Journal of Intelligent and Robotic Systems*, vol. 101, no. 21, 2021, doi: 10.1007/s10846-020-01295-w

[8] J. Yoon and J. Doh, "Optimal PID control for hovering stabilization of quadcopter using long short term memory," *Advanced Engineering Informatics*, vol. 53, no. 101679, 2022, doi: 10.1016/j.aei.2022.101679

[9] E. Paiva, J. Soto, J. Salinas and W. Ipanaqué, "Modeling, Simulation and Implementation of a modified PID Controller for stabilizing a Quadcopter", in *2016 IEEE International Conference on Automatica (ICA-ACCA)*, Curico, Chile, 2016, doi: 10.1109/ICA-ACCA.2016.7778507.

[10] E. Okyere, A. Bousbaine, G.T. Poyi, A.K. Joseph, J.M. Andrade, "LQR Controller Design for Quad-rotor Helicopters", *The Journal of Engineering*, vol. 2019, no. 17, pp. 4003-4007, 2019, doi: 10.1049/joe.2018.8126.

[11] B. Panomrattanarug, K. Higuchi, and F. Mora-Camino, ''Attitude control of a quadrotor aircraft using LQR state feedback controller with full order state observer,'' in *Proc. SICE Annu. Conf.*, 2013, pp. 2041–2046.

[12] E. Kuantama, I. Tarca, and R. Tarca, ''Feedback linearization LQR control for quadcopter position tracking,'' in *Proc. 5th Int. Conf. Control, Decis. Inf. Technol. (CoDIT)*, Apr. 2018, pp. 204–209, doi: 10.1109/CoDIT.2018.8394911

[13] A. K. Bhatia, J. Jiang, Z. Zhen, N. Ahmed, and A. Rohra, "Projection Modification Based Robust Adaptive Backstepping Control for Multipurpose Quadcopter UAV", *IEEE Access*, vol. 7, pp. 154121-154130, 2019, doi: 10.1109/ACCESS.2019.2946416

[14] H. Bouadi, M. Bouchoucha, and M. Tadjine, "Sliding Mode Control based on Backstepping Approach for an UAV Type-Quadrotor", International Journal of Mechanical and Mechatronics Engineering, vol. 1, no. 2, pp. 39-44, 2007.

[15] A. A. Mian and W. Daobo, ‘‘Modeling and backstepping-based nonlinear control strategy for a 6 DOF quadrotor helicopter,’’ *Chin. J. Aeronaut.*, vol. 21, no. 3, pp. 261–268, Jun. 2008.

[16] M. A. M. Basri, M. S. Z. Abidin, and N. A. M. Subha, ‘‘Simulation of backstepping-based nonlinear control for quadrotor helicopter,’’ *Appl. Model. Simul.*, vol. 2, no. 1, pp. 34–40, 2018.

[17] B. Zhu and D. Wang, “Nonlinear Adaptive Control Design for Quadrotor UAV Transportation System,” Drones, vol. 8, pp. 420, 2024, doi: 10.3390/drones8090420.

[18] M. Wang, B. Chen, and C. Lin, ‘‘Fixed-time Backstepping control of quadrotor trajectory tracking based on neural network,’’ *IEEE Access*, vol. 8, pp. 177092–177099, 2020. Doi: 10.1109/ACCESS.2020.3027052

[19] R. Xu and U. Ozguner, ‘‘Sliding mode control of a quadrotor helicopter,’’ in *Proc. 45th IEEE Conf. Decis. Control*, 2006, pp. 4957–4962.

[20] L. Besnard, Y. B. Shtessel, and B. Landrum, ‘‘Quadrotor vehicle control via sliding mode controller driven by sliding mode disturbance observer,’’ *J. Franklin Inst.*, vol. 349, no. 2, pp. 658–684, 2012.

[21] S. Ullah, Q. Khan, A. Mehmood, S. A. M. Kirmani, and O. Machali, ‘‘Neuro-adaptive fast integral terminal sliding mode control design with variable gain robust exact differentiator for under-actuated quadcopter UAV,’’ *ISA Transactions*, vol. 120, pp. 293–304, 2022, doi: 10.1016/j.isatra.2021.02.045.

[22] N. P. Nguyen, N. X. Mung, H. L. N. N. Thanh, T. T. Huynh, N. T. Lam, and S. K. Hong, “Adaptive sliding mode control for attitude and altitude system of a quadcopter UAV via neural network,” IEEE Access, vol. 9, pp. 40076-40085, 2021.

[23] A. Eltayeb, M. F. Rahmat, M. A. M. Basri, M. A. M. Eltoum, A. S. Elferik, “An Improved Design of an Adaptive Sliding Mode Controller for Chattering Attenuation and Trajectory Tracking of the Quadcopter UAV”, *IEEE Access*, vol. 8, pp. 205968-205979, 2020, doi: 10.1109/ACCESS.2020.3037557

[24] Y. C. Choi and H. S. Ahn, ‘‘Nonlinear control of quadrotor for point tracking: Actual implementation and experimental tests,’’ *IEEE/ASME Trans. Mechatronics*, vol. 20, no. 3, pp. 1179–1192, Jun. 2015.

[25] M. S. Esmail, M. H. Merzban, A. A. M. Khalaf, H. F. A. Hamed, and A. I. Hussein, “Attitude and altitude nonlinear control regulation of a quadcopter using quaternion representation,” *IEEE Access*, vol. 10, pp. 5884-5894, 2022. Doi: 10.1109/ACCESS.2022.3141544

[26] D. X. Ba, H. Yeom, J. Kim, and J. B. Bae, “Gain-adaptive Robust Backstepping Position Control of a BLDC Motor System,” *IEEE/ASME Trans. on Mechatronics*, vol. 23, no. 5, pp. 2470-2481, 2018.

[27] D. X. Ba, “An Intelligent Sliding Mode Controller of Robotic Manipulators with Output Constraints and High-level Adaptation,” *Int. J. Robust and Nonlinear Control*, vol. 32, no. 12, pp. 6888-6912, 2022. Doi: 10.1002/rnc.6174.

[28] A P. V. Quan, D. Xuan Ba, C. -D. Truong, N. P. Luu, V. Quang Huy and N. T. Duc, “An Adaptive Robust Nonlinear Control Approach of a Quadcopter with Disturbance Observer,” 2022 11th International Conference on Control, Automation and Information Sciences (ICCAIS), Hanoi, Vietnam, 2022, pp. 476-481, doi: 10.1109/ICCAIS56082.2022.9990185B.

[29] D. Q. Nga, D. N. Trung, “Adaptive neural network-based terminal sliding mode control for a quadrotor unmanned aerial vehicle with disturbances”, TNU Journal of Science and Technology, 2025, 230(06): pp 322-330 doi: 10.34238/tnu-jst.12556.

[30] M. Sadiq, R. Hayat, K. Zeb, A. Al-Durra and Z. Ullah, ‘‘Robust Feedback Linearization Based Disturbance Observer Control of Quadrotor UAV,’’ in IEEE Access, vol. 12, pp. 17966-17981, 2024, doi: 10.1109/ACCESS.2024.3360333.